Int. J. Heat Mass Transfer. Vol. 10, pp. 1829–1845. Pergamon Press Ltd. 1967. Printed in Great Britain

FORCED CONVECTION CONDENSATION IN THE PRESENCE OF NONCONDENSABLES AND INTERFACIAL RESISTANCE

E. M. SPARROW,* W. J. MINKOWYCZ† and M. SADDY*

(*Received* 18 *January* 1967 *and in revised form* 29 *June* 1967)

Abstract—The effect of a noncondensable gas on condensation in a forced convection laminar boundary-layer flow is explored analytically. The analysis is first carried out in general for any arbitrary flow consisting of a vapor and a noncondensable gas, and certain universal results are obtained. Solutions of the similarity differential equations are found both numerically and by an integral method. The general formulation is applied to the steam–air system, and the heat transfer with and without the noncondensable is compared for a wide range of operating conditions. The reductions in heat transfer due to the noncondensable are accentuated at low operating pressures. In general, condensation in the forced convection flow is much less sensitive than that in a gravity flow. The effect of an interfacial resistance (i.e. a temperature jump at the liquid–vapor interface) is also examined. The computed results reveal a negligible effect on the heat transfer.

NOMENCLATURE

c_p, specific heat of condensate;
D, binary diffusion coefficient;
d, diffusion layer thickness;
F, dimensionless stream function, equation (13);
f, dimensionless stream function, equation (3);
h_{fg}, latent heat;
j, diffusive mass flux;
M, molecular weight;
$\dot{m}$, interfacial mass flux;
Pr, Prandtl number of condensate;
p, total pressure;
p_v, vapor pressure;
q, surface heat flux/time-area;
R, property ratio, $[(\rho\mu)_L/(\rho\mu)]^{\frac{1}{2}}$;
Sc, Schmidt number of mixture;
T, temperature;
U_∞, free stream velocity;
u, v, velocity components;
W, mass fraction of gas;
x, y, coordinates.

Greek symbols

Δ, velocity layer thickness of mixture;
δ, condensate layer thickness;
η, similarity variable, equation (3);
η_δ, value of η at $y = \delta$;
θ, dimensionless temperature, equation (3);
μ, absolute viscosity;
ν, kinematic viscosity;
ξ, similarity variable, equation (13);
ξ_d, value of ξ at $y = d$;
ξ_Δ, value of ξ at $y = \Delta$;
ρ, density;
σ, condensation coefficient;
Φ, mass fraction variable, equation (28);
Ψ, ψ, stream functions;
Ω, interfacial resistance group, equation (41a).

* Coordenação dos Programas Pós-graduados de Engenharia, Universidade do Brasil, Rio de Janeiro.
† Department of Energy Engineering, University of Illinois at Chicago Circle, Chicago, Illinois.

Subscripts

g, condensable gas;
i, interface;
L, condensed liquid;
0, condensation of pure vapor without interfacial resistance;
w, at the wall;
∞, in the free stream;
mixture properties are unsubscripted.

INTRODUCTION

THE RECENT years have witnessed a growing interest in forced convection laminar boundary-layer flows wherein film condensation occurs [1–6]. Consideration has been given both to pure forced convection flows [2, 4] and to forced convection in the presence of a body force [1, 3, 5, 6]. In the main, these investigations were concerned with the condensation of pure saturated vapors; that is, it was assumed that noncondensable gases were not present. The possible influence of an interfacial resistance (i.e. a temperature jump at the interface between the condensate and the vapor) was also neglected.

The present paper is primarily concerned with the effect of noncondensable gases on film condensation in a forced convection laminar boundary layer. In the case of gravity-flow condensation, it has been well established both by analysis [7] and experiment [8] that the presence of a small amount of noncondensable gas gives rise to a marked reduction in the heat transfer.* Some discussion of the subject is contained in [3], but the paucity of the numerical information given therein precludes the determination of heat transfer in the presence of noncondensable gases.

Another factor which has received some attention in recent studies of gravity-flow condensation (for example [7, 9]) is the effect of a thermal resistance at the interface between the liquid and the vapor. In brief, the existence of the interfacial resistance can be traced to the fact that the net condensation of vapor is actually the difference between the simultaneous processes of evaporation and condensation. According to the kinetic theory of gases, an unbalance between these two processes must be accompanied by a temperature jump at the interface, thereby giving rise to a thermal resistance. The effect of such an interfacial resistance is also examined as part of this research.

The analytical treatment is first carried out in general and is then applied to the case wherein steam is the condensing vapor and air is the noncondensable gas. The selection of steam was made on the basis of its technical importance, and air is a common noncondensable. Results are obtained both from numerical solutions of the similarity form of the boundary-layer equations and from an integral solution (Kármán–Pohlhausen type) of the same equations. The latter solution is presented in the Appendix.

THE ANALYTICAL MODEL

The situation under study is pictured schematically in Fig. 1, which also shows dimensional nomenclature and coordinates.

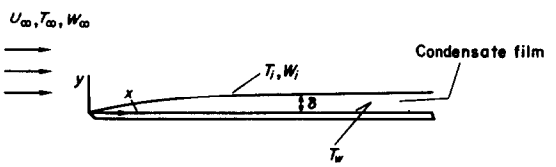

FIG. 1. Physical model and coordinate system.

The free stream flow is a mixture of a vapor and a noncondensable gas. The concentration of the noncondensable in the free stream is characterized by its mass fraction W_∞. The free stream temperature T_∞ is the saturation temperature corresponding to the partial pressure of the vapor in the free stream.

* A corresponding analytical examination for the forced convection boundary layer was, within the knowledge of the authors, unavailable at the time this investigation was performed. A relevant publication, due to Koh [12], was brought to the attention of the authors during the period of editorial review. Further discussion of Koh's contribution will be deferred until later.

The condensate layer constitutes a readily identifiable boundary layer adjacent to the plate surface. Moreover, owing to viscous, diffusion, and heat-conduction processes, velocity, concentration, and temperature boundary layers exist in the vapor–gas mixture. The dynamic interaction between the liquid and the vapor–gas boundary layers determines the rates of condensation and heat transfer.

In formulating an analytical model for the present problem, careful consideration was given to the available results for condensation of a pure vapor in a forced convection laminar boundary-layer flow [2, 4]. In the model adopted by Cess [2], inertia forces and convected energy (i.e. subcooling) are neglected in the condensate layer. In addition, the streamwise velocity at the interface is regarded as zero* for the solution of the velocity field in the vapor–gas boundary layer. On the other hand, none of these simplifications were employed by Koh [4].

The heat-transfer results from the two analyses for the Prandtl number range of non-metallic liquids (i.e. $Pr \geqslant 1$) are conveniently brought together in Fig. 8(b) of [4]. The comparison between the results must be made with considerable care owing to the values of the key parameter† $R = [(\rho\mu)_L/(\rho\mu)]^{\ddagger}$ that were employed in [4]; in particular, the lower parametric values are not realistic for typical condensation processes at atmospheric and subatmospheric pressure.‡ For realistic values of R, the results of [2, 4] are, for all practical purposes, identical; thereby lending support to the simplifying assumptions of the former analysis. Further support for the neglect of inertia and convection is provided by the order of magnitude arguments of Shekriladze [5].

When noncondensable gases are present, the condensate layer thickness is smaller than in the case of a pure vapor, all other things being equal. Correspondingly, the aforementioned simplifying assumptions become even more reasonable. Thus, in the analysis that follows, inertia and convection in the liquid layer will be neglected, and the streamwise velocity component at the interface will be taken to be zero in the computation of the velocity field in the vapor–gas boundary layer.

In addition, it is particularly convenient to consider first the case wherein noncondensable gases are present but where the interfacial resistance is neglected. The effect of the interfacial resistance is investigated in a later section of the paper.

ANALYSIS OF CONDENSATION IN THE PRESENCE OF NONCONDENSABLES

The liquid boundary layer

The starting point of the analysis is a consideration of the liquid layer. For constant fluid properties* and negligible inertia and energy convection, the conservation equations reduce to

$$\frac{\partial u}{\partial x} + \frac{\partial v}{\partial y} = 0, \qquad \frac{\partial^2 u}{\partial y^2} = 0, \qquad \frac{\partial^2 T}{\partial y^2} = 0. \quad (1)$$

Upon introducing transformed variables, these become

$$f''' = 0, \qquad \theta'' = 0 \quad (2)$$

where

$$\eta = y\sqrt{\left(\frac{U_\infty}{\nu_L x}\right)}, \qquad \psi = [\sqrt{(U_\infty \nu_L x)}]\, f(\eta),$$

$$\theta = \frac{T - T_w}{T_i - T_w}. \quad (3)$$

ψ is the conventional stream function, while T_i is the interface temperature. In general, when a noncondensable gas is present, the value of T_i is not known a *priori* but rather, it must be determined as part of the solution. The primes

* This assumption is implied when the bracketed term in Cess' equation (19c) is taken to be unity.

† Unsubscripted properties pertain to the vapor–gas mixture, while those of the liquid bear the subscript L.

‡ In the present investigation, values of R ranged from approximately 200 to 2000.

* A reference temperature will be employed when subsequent numerical evaluations are performed.

denote differentiation with respect to η. It is also useful to note that, in terms of the transformed variables, the velocity components u and v are expressible as

$$u = \frac{\partial \psi}{\partial y} = U_\infty f',$$

$$v = -\frac{\partial \psi}{\partial x} = \frac{1}{2}\left[\sqrt{\left(\frac{U_\infty \nu_L}{x}\right)}\right](\eta f' - f). \quad (4)$$

The solutions of equations (2), corresponding to the conditions that $u = v = 0$ and $T = T_w$ at the wall ($y = 0$) and that $T = T_i$ at the interface ($y = \delta$), follow readily as

$$f = \tfrac{1}{2} f''_w \eta^2, \qquad \theta = \frac{\eta}{\eta_\delta} \quad (5)$$

in which

$$f''_w = f''(0), \qquad \eta_\delta = \delta\sqrt{\left(\frac{U_\infty}{\nu_L x}\right)}. \quad (6)$$

Although equation (5) represents a formal solution of the conservation equations for the liquid layer, it is to be emphasized that both f''_w and η_δ remain to be determined.

The foregoing solution can be employed to evaluate the energy balance at the interface ($y = \delta$). Consider an element of interface (length dx) and let $\dot{m}$ be the rate at which mass crosses the interface per unit length. Under steady-state conditions, the sum of the latent heat liberated at the interface and the heat conducted to the interface from the vapor–gas side must equal the heat conducted away from the interface on the liquid side; that is

$$\dot{m} h_{fg} + k\frac{\partial T}{\partial y} = k_L\left(\frac{\partial T}{\partial y}\right)_L. \quad (7)$$

In general, the contribution of the conduction from the vapor–gas mixture is negligibly small compared with the contribution of the latent heat; correspondingly, the second term on the left-hand side of equation (7) may be omitted.

The condensation rate $\dot{m}$ is conveniently expressed in terms of the variables of the analysis by starting from the equation of definition

$$\dot{m}\,dx = \rho_L(u\,d\delta - v\,dx) \quad (8)$$

and employing equations (4) and (6), from which there follows

$$\dot{m} = \frac{1}{2}\left[\sqrt{\left(\frac{\rho_L \mu_L U_\infty}{x}\right)}\right] f(\eta_\delta). \quad (9)$$

Then, substituting this into (7) and making use of the transformed variables, one finds

$$\frac{c_p(T_i - T_w)}{h_{fg} Pr} = \frac{f(\eta_\delta)}{2\theta'(\eta_\delta)}. \quad (10)$$

Furthermore, the right-hand side can be evaluated from the solutions for f and θ, equation (5), giving

$$\frac{c_p(T_i - T_w)}{h_{fg} Pr} = \tfrac{1}{4} f''_w \eta_\delta^3. \quad (11)$$

The left-hand side of this equation represents a dimensionless group that recurs frequently in analyses of condensation, the magnitude of which governs the heat-transfer rate. Equation (11) will be employed later to eliminate the less pertinent quantity f''_w.

The velocity problem in the vapor–gas boundary layer

Strictly speaking, there are four conservation laws to be fulfilled in the vapor–gas boundary layer: mass conservation for the mixture, species conservation for one of the components, momentum conservation, and energy conservation. The latter comes into play because, owing to the presence of the noncondensable, the temperature field is nonuniform even if the free stream flow is at the saturation condition. However, as was already noted, the energy transferred to the interface due to convection–conduction in the vapor–gas boundary layer is very small relative to that liberated as latent heat. Consequently, no further consideration need be given to the energy equation.

To proceed, it is especially advantageous to deal first with the continuity and momentum

equations, and to momentarily defer treatment of the diffusion equation. The former are

$$\frac{\partial u}{\partial x}+\frac{\partial v}{\partial y}=0, \qquad u\frac{\partial u}{\partial x}+v\frac{\partial u}{\partial y}=\nu\frac{\partial^2 u}{\partial y^2} \tag{12}$$

where constant properties are assumed.* The foregoing are reduced to similarity form by writing

$$\xi=(y-\delta)\sqrt{\left(\frac{U_\infty}{\nu x}\right)} \qquad \Psi=[\sqrt{(U_\infty \nu x)}]\,F(\xi) \tag{13}$$

from which there follows

$$F'''+\tfrac{1}{2}FF''=0 \tag{14}$$

where, now, the primes represent derivatives with respect to ξ. It should be pointed out that the similarity variable is defined so that $\xi=0$ at the interface between the liquid and the vapor–gas mixture. The velocity components, when expressed in terms of the new variables, are

$$u=\frac{\partial \Psi}{\partial y}=U_\infty F' \tag{15a}$$

$$v=-\frac{\partial \Psi}{\partial x}=\frac{1}{2}\left[\sqrt{\left(\frac{U_\infty \nu}{x}\right)}\right](\xi F'-F)+U_\infty\frac{d\delta}{dx}F' \tag{15b}$$

in which the last term in equation (15b) stems from the displaced origin of the similarity variable ξ.

Equation (14) is readily recognized as the classical Blasius equation. However, the corresponding boundary conditions are altogether different from those of the Blasius case. To obtain the conditions on F, one must employ the following continuity conditions at the interface and in the free stream.

(1) The streamwise velocity u is continuous at the interface. However, owing to the fact that the interfacial value of u is very much less than U_∞, it is permissible to take $u=0$ at the interface. In view of equation (15a), this gives

$$F'(0)=0. \tag{16}$$

(2) Mass is conserved across the interface. The mass crossing the interface from the vapor–gas mixture, taking account of the diffusive as well as of the convective component, is

$$\dot{m}\,dx=\rho(u\,d\delta-v\,dx)-(j_v+j_g)\,dx \tag{17}$$

in which j_v and j_g respectively represent the diffusive fluxes of the vapor and of the gas. However, $(j_v+j_g)=0$. With this, and with the use of equations (15a) and (15b), the foregoing becomes

$$\dot{m}=\frac{1}{2}\left[\sqrt{\left(\frac{\rho\mu U_\infty}{x}\right)}\right]F(0). \tag{18}$$

Upon equating the $\dot{m}$ expressions embodied in equations (9) and (18), there follows

$$F(0)=Rf(\eta_\delta) \tag{19}$$

where

$$R=[(\rho\mu)_L/(\rho\mu)]^{\frac{1}{4}}. \tag{20}$$

(3) The shear stress $\tau=\mu(\partial u/\partial y)$ is continuous at the interface. In terms of the transformed variables, continuity of shear is expressed as

$$F''(0)=Rf''(\eta_\delta). \tag{21}$$

(4) The streamwise velocity u approaches U_∞ as y approaches infinity. In light of equation (15a), this condition takes the form

$$F'(\infty)=1. \tag{22}$$

The four conditions on F, as represented by equations (16, 19, 21, 22), can be rephrased and simplified by employing already derived results for the liquid layer. In particular, the $f(\eta_\delta)$ and $f''(\eta_\delta)$ appearing in equations (19) and (21) can be eliminated with the aid of (5) and subsequently, in its turn, f''_w is eliminated by employing equation (11). As a result of these operations,

* The accounting of variable fluid properties would immediately require that consideration be given to specific fluids and to specific operating conditions, thereby destroying the generality of the present solution method. It is the intention of the authors to examine the effect of fluid property variations at a later time.

the conditions on F can be stated as

$$F(0) = \left[R\frac{c_p(T_i - T_w)}{h_{fg}Pr}\right]\frac{2}{\eta_\delta}, \qquad F'(0) = 0,$$

$$F''(0) = \left[R\frac{c_p(T_i - T_w)}{h_{fg}Pr}\right]\frac{4}{\eta_\delta^3}. \tag{23a}$$

$$F'(\infty) = 0. \tag{23b}$$

Furthermore, from equations (23a), it is apparent that

$$R\frac{c_p(T_i - T_w)}{h_{fg}Pr} = \left\{\frac{[F(0)]^3}{2F''(0)}\right\}^{\frac{1}{4}} \tag{24a}$$

$$\eta_\delta = \left[\frac{2F(0)}{F''(0)}\right]^{\frac{1}{4}}. \tag{24b}$$

Indeed, equations (24a) and (24b) may be regarded as alternatives to the first and third boundary conditions appearing in (23a), and it is, in fact, especially convenient to do so.

In light of the fact that equation (14) is of third order, it is sufficient to prescribe three boundary conditions to specify its solution. Let these be $F(0) = \text{constant} \geqslant 0$, $F'(0) = 0$, and $F'(\infty) = 1$. For a given $F(0)$, a numerical solution of equation (14) can be performed. Such a solution provides, among other results, the value of $F''(0)$. Then, using the prescribed $F(0)$ and the calculated $F''(0)$, the corresponding values of $R[c_p(T_i - T_w)/h_{fg}Pr]$ and η_δ can be evaluated from equations (24a) and (24b). By assigning a sequence of values of $F(0)$, the relationship between the aforementioned parameters can be mapped out.

As a matter of good fortune, Emmons and Leigh [10] have already numerically solved equation (14) for a large number of $F(0)$ values between 0 and 10. The $F(0)$ and $\phi''(0)$ are listed in Table 1 along with the corresponding values of $R[c_p(T_i - T_w)/h_{fg}Pr]$ and η_δ^{-1}. These latter quantities are also plotted in Fig. 2 (solid line).

There are several observations which are relevant to Fig. 2 and Table 1. First of all, the results have a universal character, that is, there is not a separate dependence of η_δ on R and on $c_p(T_i - T_w)/h_{fg}Pr$; rather, only the product of these parameters appears. This is in contrast to the case of gravity-flow condensation, where, even if similar simplifying assumptions are made,

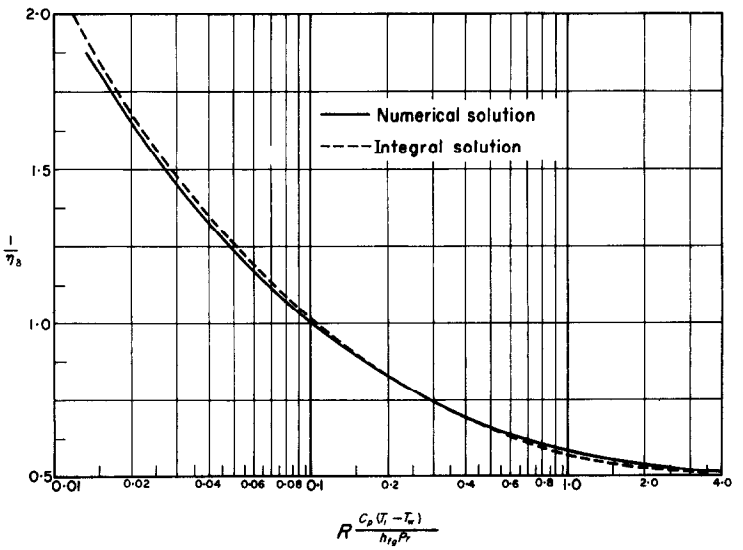

FIG. 2. Variation of $1/\eta_\delta$ with $Rc_p(T_i - T_w)/h_{fg}Pr$.

a comparable universal representation cannot be achieved. The condensation rate increases with increasing values of the abscissa of Fig. 2, while the ordinate represents the inverse of the condensate layer thickness δ. Therefore, the thickness of the condensate layer increases with the condensation rate, but the increase is very gradual for larger abscissa values; this fact will be of significance in the numerical evaluations of the heat-transfer rate that will be made in a later section. At large values of the abscissa, $1/\eta_\delta$ approaches 0·5, while for small values of the abscissa,

$$\frac{1}{\eta_\delta} \sim \left[\frac{0{\cdot}332}{4}\Big/ R\frac{c_p(T_i - T_w)}{h_{fg}\,Pr}\right]^{\frac{1}{4}}. \qquad (25)$$

Table 1. Results from the velocity and diffusion solutions*

$F(0)$	$F''(0)$	$R\frac{c_p(T_i - T_w)}{h_{fg}\,Pr}$	$\frac{1}{\eta_\delta}$	$\frac{W_\infty}{W_i}$
0·05	0·35026	0·013358	1·87150	0·95073
0·10	0·36867	0·036827	1·35770	0·90510
0·15	0·38730	0·066008	1·13620	0·86273
0·20	0·40612	0·099244	1·00760	0·82332
0·25	0·42514	0·13556	0·92210	0·78658
0·30	0·44434	0·17431	0·86053	0·75225
0·35	0·46371	0·21501	0·81391	0·72013
0·40	0·48325	0·25733	0·77721	0·69002
0·45	0·50296	0·30098	0·74755	0·66175
0·50	0·52282	0·34575	0·72306	0·63517
0·60	0·56300	0·43799	0·68494	0·58654
0·70	0·60373	0·53298	0·65668	0·54321
1·00	0·72887	0·82825	0·60368	0·43803
1·50	0·94542	1·3360	0·56138	0·31857
2·00	1·16943	1·8495	0·54069	0·24075
3·00	1·63223	2·8759	0·52157	0·14927
4·00	2·10740	3·8967	0·51325	0·10047
5·00	2·58990	4·9125	0·50890	0·07173
6·00	3·07708	5·9244	0·50638	0·05322
10·00	5·04852	9·9518	0·50242	0·02161

* For $Sc = 0{\cdot}55$

If the interface temperature T_i were known, then Fig. 2 (or Table 1) would contain all the information needed to calculate the rate of heat transfer. However, T_i is unknown, and a consideration of the diffusion processes in the vapor gas mixture is necessary for its determination.

The diffusion problem

Let W denote the local mass fraction of the noncondensable gas such that

$$W = \rho_g/(\rho_g + \rho_v). \qquad (26)$$

Species conservation for the noncondensable gas can then be expressed by a diffusion equation as follows

$$\rho u\frac{\partial W}{\partial x} + v\frac{\partial W}{\partial y} = D\frac{\partial^2 W}{\partial y^2} \qquad (27)$$

in which D is the binary diffusion coefficient. By making use of the similarity transformation, equations (13) and (15), and introducing a reduced mass fraction Φ

$$\Phi = \frac{W - W_\infty}{W_i - W_\infty} \qquad (28)$$

the diffusion equation can be rephrased as

$$\Phi'' + \tfrac{1}{2}Sc\,F\Phi' = 0. \qquad (29)$$

The quantities W_i and W_∞ are, respectively, the mass fractions of the noncondensable gas at the interface and in the free stream. Whereas W_∞ may be regarded as known, W_i is not known *a priori*. Sc denotes the Schmidt number of the mixture. The boundary conditions on Φ follow directly from equation (28), thus

$$\Phi(0) = 1, \qquad \Phi(\infty) = 0. \qquad (30)$$

A formal solution of equations (29) and (30) can be written in the form

$$\Phi(\xi) = 1 - \int_0^\xi \exp\left(-\frac{Sc}{2}\int_0^\xi F\,d\xi\right) \times d\xi \Big/ \int_0^\infty \exp\left(-\frac{Sc}{2}\int_0^\xi F\,d\xi\right)d\xi. \qquad (31)$$

Of particular relevance for the present analysis is the derivative $d\Phi/d\xi$ at $\xi = 0$, which follows from equation (31) as

$$\Phi'(0) = -1\Big/\int_0^\infty \exp\left(-\frac{Sc}{2}\int_0^\xi F\,d\xi\right)d\xi. \qquad (32)$$

It remains to extract the value of the interfacial mass fraction W_i, which, in turn, leads to the interface temperature T_i. Owing to the fact that the interface is impermeable to the noncondensable gas, it follows that the interfacial mass flux of the noncondensable is zero. Taking cognizance of both convective and diffusive transport, the impermeability condition becomes

$$\rho_g\left(u\frac{\mathrm{d}\delta}{\mathrm{d}x}-v\right)=j_g=-\rho D\frac{\partial W}{\partial y}. \quad (33)$$

If equation (33) is recast into the variables of the analysis, one arrives at

$$1-\frac{W_\infty}{W_i}=-\frac{F(0)Sc}{2\Phi'(0)}. \quad (34)$$

Sc, $F(0)$, and $\Phi'(0)$ thus available, equation (34) yields W_∞/W_i. By successively prescribing $F(0)$, a corresponding set of values for W_∞/W_i can be generated. However, since there is a unique relationship between $F(0)$ and $R[c_p(T_i-T_w)/h_{fg}Pr]$, it follows that W_∞/W_i is also uniquely related to the latter parameter, for a given Schmidt number.

In anticipation of the forthcoming heat-transfer calculations, W_∞/W_i has been evaluated for $Sc = 0{\cdot}55$ (mixture of air and steam). The results are listed in the last column of Table 1 and are also plotted in Fig. 3. It is evident that for all cases, $W_i \geqslant W_\infty$; in other words, there is a buildup of noncondensable gas at the interface. Moreover, if it is recognized that the abscissa is a measure of the condensation rate,

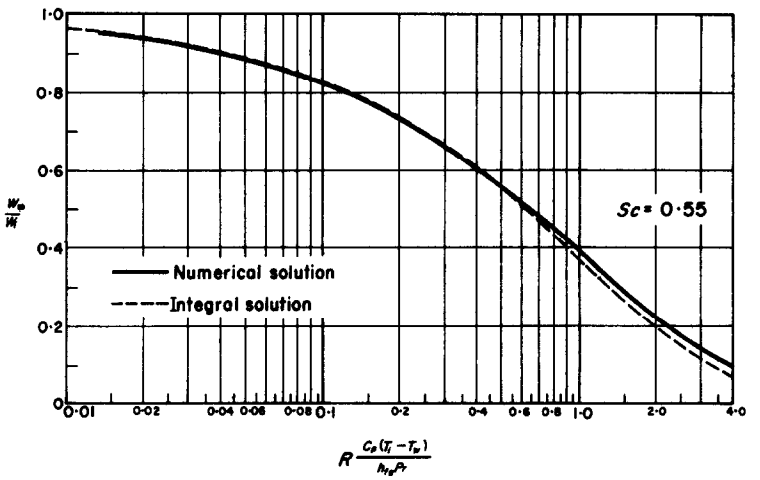

FIG 3. Variation of W_∞/W_i with $Rc_p(T_i - T_w)/h_{fg}Pr$ for $Sc = 0{\cdot}55$.

It is interesting to observe that W_∞ and W_i appear only as the quotient W_∞/W_i.

Now, attention may be turned to the determination of W_i. First, the Schmidt number is specified for the vapor–gas mixture under consideration. Then, if $F(0)$ is also specified, the function $F(\xi)$ is known and the quadrature represented by equation (32) yields $\Phi'(0)$. With then it is evident from Fig. 3 that the buildup is accentuated at high rates of condensation. Indeed, the interfacial mass fraction of the noncondensable may exceed the free stream value by a factor of 10 or 20.

The aforementioned trend is reasonable on physical grounds. A higher condensation rate is associated with a larger convective flow

toward the interface. The convective flow carries noncondensable gas as well as vapor. To balance the larger convective inflow of the noncondensable, there must be a correspondingly augmented diffusive outflow. The magnitude of the diffusive flow depends on the magnitude of the concentration gradient, whence the increase of the interfacial mass fraction.

Aside from the separate dependence on the Schmidt number, the results appearing in Fig. 3 have a remarkably universal character. In particular, the single W_∞/W_i curve is universal for all W_∞. Furthermore, as was already discussed in connection with Fig. 2, the dependence on R and $c_p(T_i - T_w)/h_{fg}\,Pr$ appears only as a product of these parameters. In contrast, it is interesting to observe that for gravity-flow condensation, W_∞/W_i depends separately on Sc, W_∞, R, and $c_p(T_i - T_w)/h_{fg}\,Pr$.

The procedure by which the W_i results are employed in determining the interface temperature T_i will now be outlined.

Interface temperature; heat transfer

Consider the condensation problem involving a specific vapor and noncondensable gas wherein the following quantities are specified: T_∞, W_∞, T_w. This information, coupled with the results presented in the prior section, is sufficient for the determination of the interface temperature T_i.

The first step is to evaluate the total pressure p of the system. For this purpose, it is convenient to assume that the mixture and its components behave like perfect gases such that

$$\frac{p_v}{p} = \frac{1 - W}{1 - W(1 - M_v/M_g)} \tag{35}$$

where p_v represents the vapor pressure. If T_∞ is specified and the free stream is assumed to be at saturation, then p_v is available from the tabulated properties of the vapor. With this and with the known value of W_∞, the total pressure p follows from equation (35).

Next, a trial value of T_i is assumed. Owing to the fact that the interface is a saturation state for the vapor, the choice of T_i also fixes p_{vi}. With these, W_i is found from the relation

$$W = \frac{1 - (p_v/p)}{1 - (p_v/p)(1 - M_v/M_g)} \tag{36}$$

which is simply a rephrasing of equation (35).

Attention may now be turned to evaluating the abscissa variable of Fig. 3. For this purpose, the thermodynamic and transport properties (R, c_p, h_{fg}, Pr) appearing therein are calculated at interface conditions. With these and with $(T_i - T_w)$, the value of the abscissa is determined and W_∞/W_i is read from the curve. The resulting W_i is converted to p_{vi} by applying equation (35) and, in turn, T_i follows from the tabulated saturation data for the vapor. If the T_i thus obtained differs from that originally assumed, a readjustment is made and the process is repeated until convergence is achieved.

The procedure outlined above can be modified to shorten the computations. For instance, for a given W_∞, the W_∞/W_i curve of Fig. 3 can be converted to a p_{vi}/p curve, thereby eliminating further consideration of W_i. However, more significantly, the entire procedure can be carried out on an electronic computer. Indeed, the forthcoming numerical results of this investigation were generated in this manner.

Once T_i has been found, then the heat-transfer rate follows directly. Let q denote the local heat transferred to the surface per unit time and unit area, so that

$$q = k_L\left(\frac{\partial T}{\partial y}\right)_{y=0} = \frac{k_L(T_i - T_w)}{\eta_\delta}\sqrt{\left(\frac{U_\infty}{\nu_L x}\right)} \tag{37}$$

where equations (3) and (5) have also been used. The quantity $1/\eta_\delta$ is a unique function of $R[c_p(T_i - T_w)/h_{fg}\,Pr]$, and T_i is calculated as described in the foregoing paragraphs.

It is particularly interesting to compare the heat-transfer rate in the presence of noncondensables with that for the case of a pure vapor. The comparison is made under the condition that T_∞, T_w, and U_∞ are the same in the

two cases. For the pure vapor (subscript 0), one has

$$q_0 = \frac{k_{L,0}(T_\infty - T_w)}{\eta_{\delta,0}} \sqrt{\left(\frac{U_\infty}{\nu_{L,0}x}\right)} \quad (38)$$

where $\eta_{\delta,0}$ is found from Fig. 2 by replacing $(T_i - T_w)$ in the abscissa with $(T_\infty - T_w)$ and evaluating the fluid properties at T_∞. Then, upon ratioing equations (37) and (38), there follows

$$\frac{q}{q_0} = \left(\frac{1/\eta_\delta}{1/\eta_{\delta,0}}\right)\left(\frac{T_i - T_w}{T_\infty - T_w}\right)\left(\frac{k_L}{k_{L,0}}\right)\sqrt{\left(\frac{\nu_{L,0}}{\nu_L}\right)}. \quad (39)$$

The ratios of the condensate layer thicknesses and the temperature differences that constitute the first two terms of equation (39) are evaluated in accordance with the foregoing development. It only remains to discuss the computation of the property ratios. When a constant-property analysis is applied to a real fluid, it is common to take account of the temperature-dependence of the properties by employing a reference temperature. For the two cases under consideration here, the corresponding reference temperatures may be represented as

$$T^* = T_w + C(T_i - T_w) \quad (40a)$$

$$T_0^* = T_w + C(T_\infty - T_w). \quad (40b)$$

The constant C has not been determined specifically for the problem of forced convection condensation. However, owing to the fact that the temperature differences are not large and that only property ratios are involved, there is no need to know C to a high degree of precision. For the case of gravity-flow condensation, the value of C was found to be 0·31. For present purposes, it was deemed sufficient to use $C = \frac{1}{3}$.

Summing up, it is seen that for prescribed values of T_∞, T_w, and W_∞, the heat-transfer ratio q/q_0 can be calculated for a given free stream flow of vapor and noncondensable gas. The departure of q/q_0 from unity is direct measure of the effect of the noncondensable gas.

The just-concluded general development will now be applied to the case of steam with air as the noncondensable.

CONDENSATION OF STEAM WITH AIR AS NONCONDENSABLE

The steam–air system, besides being of engineering interest, offers the possibility of direct comparison between forced convection boundary-layer flow (present investigation) and gravity flow [7]. The specialization of the solution method described in the preceding sections to a given vapor–gas system can be made as soon as the appropriate fluid properties are assembled. These include properties of the pure vapor (including the vapor pressure–temperature relation), of the condensed liquid, and of the gas. In addition, expressions for computation of the mixture density and viscosity are needed, as is the mixture Schmidt number. The fluid properties for the steam–air system that were used in this investigation are the same as those previously employed in [7]. Inasmuch as the sources of the property data and the computation methods pertaining thereto are adequately discussed in the reference, there is no need for repetition here.

Computations of q/q_0 were performed for five values of the free stream temperature T_∞ ranging from 212 to 80°F, which correspond approximately to a range in the system pressure p from 1 atmosphere to 0·5 psi. At each T_∞, the mass fraction W_∞ of the air in the free stream was assigned values of 0·005, 0·02, 0·05 and 0·10. In addition, at each fixed W_∞, the temperature difference $(T_\infty - T_w)$ was varied between 2 degF and 40 degF.

The heat-transfer results are presented in Figs. 4–8, which correspond respectively to T_∞ values of 212, 180, 150, 115 and 80°F. In each figure, q/q_0 is plotted as a function of the temperature difference $(T_\infty - T_w)$ for parametric values of W_∞. The solid lines represent the results for forced convection condensation. The departure of the curves from unity is a direct measure of the effect of the noncondensable gas.

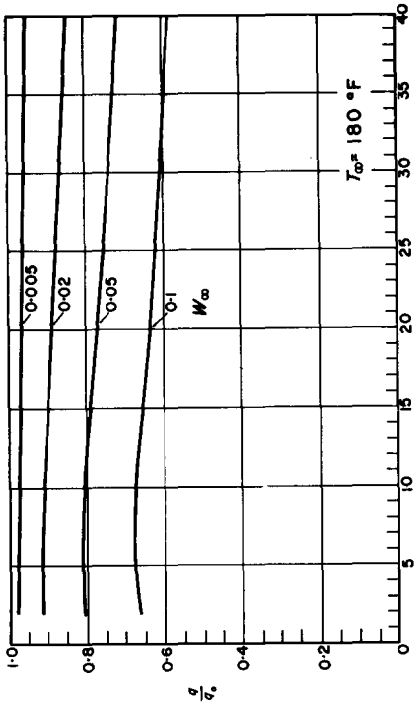

FIG. 5. Condensation heat transfer for steam–air system, $T_\infty = 180°F$.

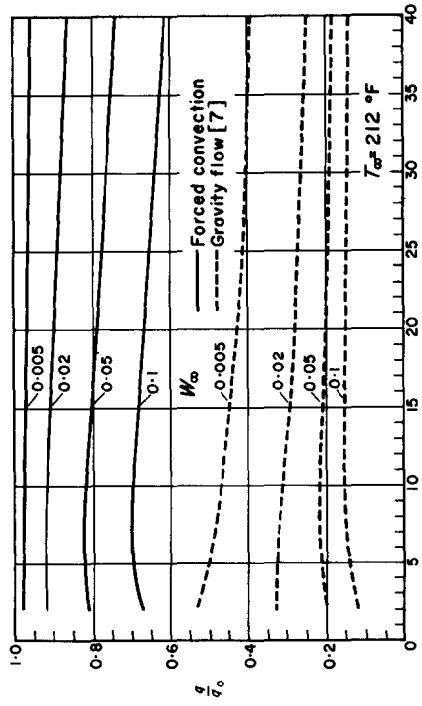

FIG. 4. Condensation heat transfer for steam–air system, $T_\infty = 212°F$.

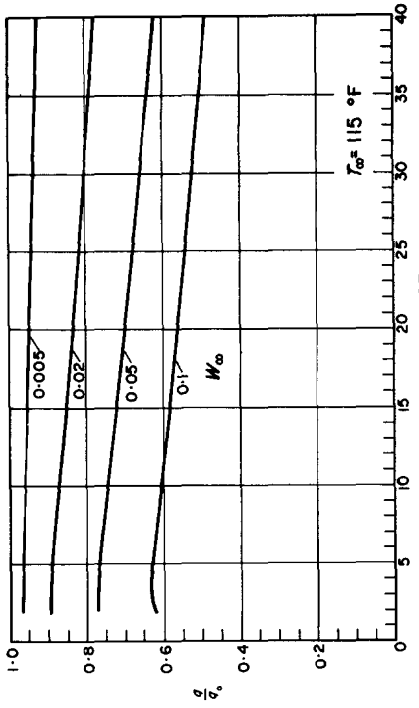

FIG. 7. Condensation heat transfer for steam–air system, $T_\infty = 115°F$.

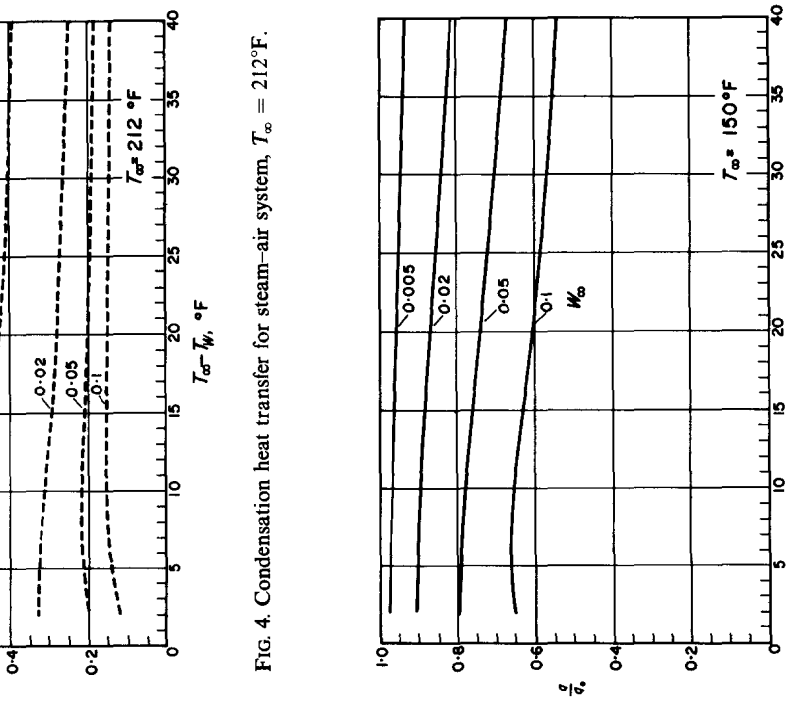

FIG. 6. Condensation heat transfer for steam–air system, $T_\infty = 150°F$.

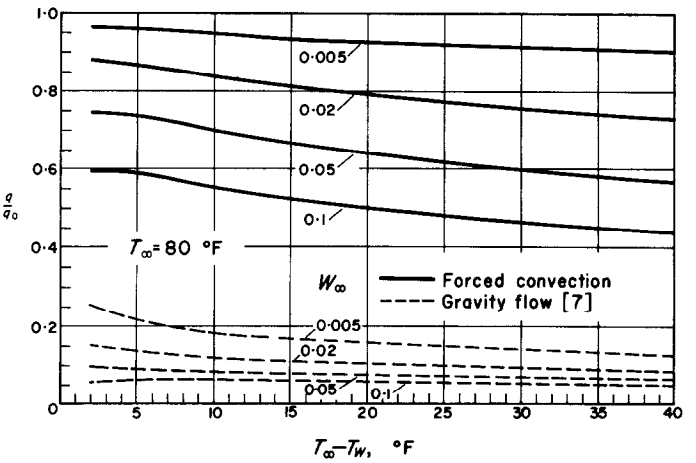

FIG. 8. Condensation heat transfer for steam–air system, $T_\infty = 80°F$.

Inspection of the figures reveals several general trends. At any fixed temperature difference and fixed free stream temperature level, the heat transfer decreases monotonically as the mass fraction of the noncondensable increases. The decrease in heat transfer is perceptibly accentuated as the free stream temperature decreases (for instance, compare Figs. 4 and 8). Thus, the presence of the noncondensable is more strongly manifested when the condensation takes place at sub-atmospheric pressures. At the higher free stream temperature levels and at the lower mass fractions, q/q_0 is rather insensitive to the temperature difference $(T_\infty - T_w)$. When T_∞ decreases and W_∞ increases, the heat-transfer ratio becomes more sensitive to the temperature difference, decreasing as $(T_\infty - T_w)$ increases.

Perhaps as interesting as the aforementioned trends are the actual magnitudes of the reductions in heat transfer. For a trace amount of noncondensable gas, say $W_\infty = 0{\cdot}005$, the heat transfer is only slightly decreased. Indeed, even for $W_\infty = 0{\cdot}02$, appreciable effects are encountered only at the lower temperature levels and larger temperature differences. With larger values of W_∞, such as $0{\cdot}10$, q/q_0 is much less than unity, especially at low temperature levels.

The just-described decreases in the heat-transfer rate can be attributed to the buildup of the noncondensable gas at the interface, as was already discussed in connection with Fig. 3. The effect of such a buildup is to lower the corresponding partial pressure of the vapor, which, in turn, lowers the interface temperature T_i at which the condensation occurs (the interface is a saturation state). In this way, the thermal driving force $(T_i - T_w)$ is lowered, thereby decreasing the heat-transfer rate.

It is especially interesting to compare the effect of the noncondensable gas in forced convection condensation with that for gravity-flow condensation. Results for the latter situation, available from [7], are plotted in Figs. 4 and 8 as dashed lines.* Inspection of the gravity-flow results indicates general trends that are essentially the same as those already enumerated for the forced-convection case. However, there is a dramatic difference in the extent of the heat-transfer reductions brought about by the presence of the noncondensable gas. It is clear that gravity-flow condensation is very much more

* Although available, gravity-flow results are not included in Figs. 5–7 because such further comparisons yield conclusions identical to those which follow from Figs. 4 and 8.

sensitive to a noncondensable gas than is forced convection condensation, a finding that is intuitively reasonable. Indeed, in the former case, the presence of trace amounts ($W_\infty = 0{\cdot}005$) can lead to q/q_0 values on the order of 0·4–0·2, while larger concentrations such as $W_\infty = 0{\cdot}10$ can reduce q/q_0 to 0·1. These values of q/q_0 are significantly lower than those for the forced convection case.

It is also appropriate to discuss the work of Koh [12]. This publication describes a method for calculating the effect of noncondensables on forced convection film condensation; but, aside from a single isolated case, no heat-transfer results are given. Owing to the fact that Koh elected to treat the problem without making use of the judicious simplifications employed here, his approach requires the pre-tabulation of information which depends on four independent parameters (rather than the present two). In light of such an extensive parametric dependence, it is not surprising that a pre-tabulation would fail to cover a significant number of interesting cases. For instance, none of the results appearing in Figs. 4–8 of the present paper is calculable from the information provided by Koh. In addition, no suggestion appears in Koh's work as to how to select the parameters Pr and R, the choice apparently being somewhat arbitrary. Thus, in the one case worked out by Koh, Pr and R were taken as 1 and 100, about half of the appropriate values.

The single case considered by Koh for condensation involving a steam–air mixture is for $W_\infty = 0{\cdot}02$ and $T_\infty = 212°\text{F}$ (saturation temperature of free stream flow), along with Pr and R values as noted above. Unfortunately, no information is given about T_w, and this precludes the possibility of direct comparison with the present results. However, there is every indication that the $T_\infty - T_w$ corresponding to Koh's computation was very much larger than any investigated here. This is inferred from the fact that Koh gives a value for T_i of 190°F while the T_i corresponding to the rightmost point on the $W_\infty = 0{\cdot}02$ curve of Fig. 4 is approximately 207°F. For his assigned conditions, Koh finds $q/q_0 = 0{\cdot}795$, which is substantially below any of the values appearing in Fig. 4 for $W_\infty = 0{\cdot}02$. On the basis of his single result, Koh inferred that the effects of noncondensables in forced convection and gravity flows were of comparable magnitude. This inference is not borne out by the extensive comparisons of Figs. 4 and 8.

THE EFFECT OF AN INTERFACIAL RESISTANCE

As explained in the Introduction, kinetic theory indicates that the temperature of a condensing vapor differs from the temperature of the adjacent condensed phase. The effect of such a jump phenomenon is to lower the interface temperature, thereby reducing the thermal driving force. The magnitude of the temperature jump varies directly with the rate of condensation; consequently, the interfacial resistance is most strongly manifested in the case of a pure vapor, as was verified by heat-transfer calculations for gravity-flow condensation [7]. In view of this, the forthcoming discussion will be concerned only with a pure vapor.

A widely accepted representation for the temperature jump, specialized to the case of a pure, saturated vapor (for instance, [9]), is

$$\dot{m} = \Omega(T_\infty - T_i) \tag{41}$$

where

$$\Omega = \left(\frac{\sigma}{2-\sigma}\right)\left(\frac{2}{\pi R^3}\right)^{\frac{1}{2}} \frac{h_{fg}p_\infty}{T_\infty^{\frac{3}{2}}}. \tag{41a}$$

In the foregoing, σ is the condensation coefficient characterizing the fraction of the vapor molecules striking the liquid surface which actually condense. R is the gas constant of the vapor.

The numerical values of σ are different for different fluids. Indeed, even for a given fluid, the values of σ reported by various investigators show considerable variation. For water,

which has been subject to rather intensive investigation, σ values ranging from 0·04 to 1 have been reported. The most recent measurements, performed with great care, indicate that σ is at least 0·35 and is probably unity. The various literature sources wherein this information is contained are cited in [7] and will not be repeated here.

The mass flux passing from the vapor into the interface is also expressed by equation (18). Upon equating the $\dot{m}$ expressions from equations (41) and (18), there follows, after rearrangement

$$\frac{T_\infty - T_w}{T_i - T_w} = 1 + \left[\frac{\rho U_\infty F(0)}{2\Omega(T_i - T_w)}\Big/\sqrt{\left(\frac{U_\infty x}{\nu}\right)}\right]. \quad (42)$$

Equation (42) provides a means for computing the change in the thermal driving force owing to the effect of the interfacial resistance. Once the foregoing ratio of temperature differences is known, the reduction in heat transfer can be evaluated by applying equation (39), where now the unsubscripted and subscripted quantities respectively denote the cases with and without interfacial resistance.

It is evident from equation (42) that the values of U_∞, x, T_∞, $(T_i - T_w)$ and σ, as well as the fluid itself, must be specified before the computations can be performed. Values of 20 ft/s and 0·25 ft appear to be reasonable choices for U_∞ and x. Then, for $T_\infty = 212°F$ and $(T_i - T_w) = 40$ degF, q/q_0 was found to be 0·9997, 0·9985 and 0·985, respectively for $\sigma = 1$, 0·35 and 0·04. These results are essentially unchanged when the computations were repeated using $(T_i - T_w) = 5$ degF. Next, the heat transfer was computed for a temperature level $T_\infty = 80°F$, resulting in $q/q_0 = 0·997$, 0·987 and 0·873 for $\sigma = 1·0$, 0·35 and 0·04. These values are very little different if $(T_i - T_w) = 40$ degF or 5 degF.

Only if the σ value were 0·04 would the interfacial resistance lead to a non-negligible reduction in heat transfer and then only at the relatively low temperature level $T_\infty = 80°F$. In light of recent evidence suggesting that $\sigma = 1$ for steam, it may be concluded that the interfacial resistance has a negligible effect on forced convection condensation for this fluid. This is in accordance with the findings of [7] for the case of gravity-flow condensation.

ACKNOWLEDGEMENTS

This research was, in part, supported by the National Science Foundation under Grant No. GK-844. Their support is gratefully acknowledged. The authors also wish to thank Shu Chien Yung for programming the computer calculations.

REFERENCES

1. W. M. ROHSENOW, J. H. WEBBER and A. T. LING, Effect of vapor velocity on laminar and turbulent film condensation, *Trans. Am. Soc. Mech. Engrs* **78**, 1637–1643 (1956).
2. R. D. CESS, Laminar film condensation on a flat plate in the absence of a body force, *Z. Angew. Math. Phys.* **11**, 426–433 (1960).
3. P. M. CHUNG, Film condensation with and without body force in a boundary layer flow of vapor over a flat plate, NASA TN D-790 (1961).
4. J. C. Y. KOH, Film condensation in a forced-convection boundary layer flow, *Int. J. Heat Mass Transfer* **5**, 941–954 (1962).
5. I. G. SHEKRILADZE and V. I. GOMELAURI, Theoretical study of laminar film condensation of flowing vapor, *Int. J. Heat Mass Transfer* **9**, 581–591 (1966).
6. H. R. JACOBS, An integral treatment of combined body force and forced convection film condensation, *Int. J. Heat Mass Transfer* **9**, 637–648 (1966).
7. W. J. MINKOWYCZ and E. M. SPARROW, Condensation heat transfer in the presence of noncondensables, interfacial resistance, superheating, variable properties, and diffusion, *Int. J. Heat Mass Transfer* **9**, 1125–1144 (1966).
8. D. F. OTHMER, The condensation of steam, *Ind. Engng Chem.* **21**, 577–583 (1929).
9. S. P. SUKHATME and W. M. ROHSENOW, Heat transfer during film condensation of a liquid metal vapor, *J. Heat Transfer* **88**, 19–28 (1966).
10. H. W. EMMONS and D. C. LEIGH, Tabulation of the Blasius function with blowing and suction, Fluid Motion Sub-Committee, Aeronaut. Res. Coun., Report No. FM 1915 (1953).
11. M. SADDY, Condensação no presenca de não condensavel em fluxo forcado, M.Sc. thesis, Coordenação dos Programas Pos-Graduados de Engenharia, Universidade do Brasil, Rio de Janeiro, Brasil (1966).
12. J. C. Y. KOH, Laminar film condensation of condensable gases and gaseous mixtures on a flat plate, in *Proceedings of the 4th National Congress of Applied Mechanics*, pp. 1327–1336 (1962).

APPENDIX

Integral Solution for Condensation in the Presence of a Noncondensable

An alternate, but approximate, solution for forced convection condensation in the presence of a noncondensable gas can be carried out using the momentum and diffusion integrals [11]. By making liberal reference to the formulation reported in the main body of the paper, the description of the integral solution can be kept brief.

The analysis of the liquid layer remains the same as before. To solve the velocity problem in the vapor–gas layer, equation (14) is replaced by its integral form

$$2F''(0) = F(0)[1 - F'(0)] + \int_0^{\xi_\Delta} F'\mathrm{d}\xi - \int_0^{\xi_\Delta} (F')^2\mathrm{d}\xi \tag{43}$$

wherein

$$\xi_\Delta = (\Delta - \delta)\sqrt{\left(\frac{U_\infty}{\nu x}\right)} \tag{44}$$

and $y = \Delta$ represents the edge of the velocity boundary layer in the vapor–gas mixture. For the velocity profile, one may use

$$F'(\xi) = 2\left(\frac{\xi}{\xi_\Delta}\right) - \left(\frac{\xi}{\xi_\Delta}\right)^2. \tag{45}$$

The foregoing satisfies the conditions that $F'(0) = 0$, $F'(\xi_\Delta) = 1$, $F''(\xi_\Delta) = 0$. Moreover, by subjecting equation (45) to the third of conditions (23a), one finds

$$\xi_\Delta = \eta_\delta^3 \Big/ 2\left[R\frac{c_p(T_i - T_w)}{h_{fg}Pr}\right] \tag{46}$$

thereby establishing a relation between ξ_Δ and η_δ.

Then, upon substituting the profile (45) into the integrated momentum equation (43), carrying out the integrations, and making use of (46) and (23), there follows

$$\frac{\eta_\delta^6}{4 - \eta_\delta^2} = 30\left[R\frac{c_p(T_i - T_w)}{h_{fg}Pr}\right]^2. \tag{47}$$

In effect, equation (47) takes the place of equation (24a) and the first two columns of Table 1.

Numerical results obtained by solving equation (47) are listed in Table A1 and are also plotted in Fig. 2 (dashed line). Inspection of the figure shows that good agreement exists between the approximate and the exact solutions.

Table A1. *Results from the integral solution*

$R\frac{c_p(T_i - T_w)}{h_{fg}Pr}$	$\frac{1}{\eta_\delta}$	$\frac{\xi_\Delta}{\xi_d}$	$\frac{W_\infty}{W_i}$
0·0103	2·092	0·795	0·9606
0·0210	1·658	0·793	0·9371
0·0334	1·429	0·790	0·9149
0·0510	1·250	0·786	0·8880
0·105	1·000	0·777	0·8230
0·169	0·870	0·766	0·7627
0·228	0·800	0·756	0·7156
0·352	0·714	0·737	0·6344
0·466	0·667	0·724	0·5729
0·624	0·625	0·707	0·5021
0·852	0·588	0·685	0·4198
1·221	0·556	0·657	0·3212
1·521	0·541	0·639	0·2627
2·304	0·521	0·606	0·1636
3·460	0·510	0·581	0·0912

Next, attention is directed to the diffusion equation (29), whose integral form may be written as

$$2\Phi'(0) = -Sc\left[F(0) + \int_0^{\xi_d} \Phi F'\mathrm{d}\xi\right] \tag{48}$$

where

$$\xi_d = (d - \delta)\sqrt{\left(\frac{U_\infty}{\nu x}\right)} \tag{49}$$

and $y = d$ is the thickness of the diffusion layer. A mass fraction profile satisfying the conditions $\Phi(0) = 1$, $\Phi(\xi_d) = 0$, $\Phi'(\xi_d) = 0$ is

$$\Phi(\xi) = 1 - 2\left(\frac{\xi}{\xi_d}\right) + \left(\frac{\xi}{\xi_d}\right)^2. \tag{50}$$

Also, by making use of the impermeability condition (34) and the first of equations (23a),

one finds

$$\xi_d = 2\eta_\delta\left(1 - \frac{W_\infty}{W_i}\right)\Big/ Sc\left[R\frac{c_p(T_i - T_w)}{h_{fg}Pr}\right]. \tag{51}$$

The integration appearing in equation (48) may now be performed. In this connection, it is essential to note that for the Schmidt number of interest here (0·55), $\xi_d > \xi_\Delta$. Upon taking cognizance of this fact and carrying out the indicated operations, there results

$$\frac{W_\infty}{W_i} = \frac{1}{12}Sc\xi_d^2\left[1 - \left(\frac{\xi_\Delta}{\xi_d}\right) + \frac{1}{2}\left(\frac{\xi_\Delta}{\xi_d}\right)^2 - \frac{1}{10}\left(\frac{\xi_\Delta}{\xi_d}\right)^3\right]. \tag{52}$$

For a given Schmidt number, the determination of W_∞/W_i is carried out on a trial and error basis for a selected value of $R[c_p(T_i - T_w)/h_{fg}Pr]$. Corresponding to the latter, equations (47) and (46) respectively give η_δ and ξ_Δ. Then, upon assuming a trial value of W_∞/W_i, ξ_d is calculated from (51). With the known values of ξ_Δ and ξ_d, a new W_∞/W_i is obtained from equation (52). If the output and input values of W_∞/W_i are not the same, another guess is made and equations (51) and (52) are re-evaluated. This procedure is repeated until convergence is achieved.

The results of the aforementioned calculation procedure are listed in Table A1, and the W_∞/W_i are also plotted in Fig. 3 (dashed line). In general, the agreement between the two curves shown in the figure is satisfactory, with the greatest deviations occuring at the larger values of the abscissa.

The results from the integral solution were employed as a basis for computing q/q_0 curves corresponding to the conditions of Figs. 4 and 8. The general agreement of these results with those shown in the aforementioned figures is entirely satisfactory, but there are some small differences in detail. These differences presumably stem, at least partially, from the deviations between the W_∞/W_i curves shown in Fig. 3. However, part of the difference may well be due to the fact that the fluid properties used in computing the q/q_0 results from the integral solution were somewhat different from those used in evaluating the exact solution. In view of the uncertainty introduced by the use of different fluid properties, the q/q_0 results from the integral solution have not been included in Figs. 4 and 8.

Résumé—L'effet d'un gaz non condensable sur la condensation avec convection forcée dans une couche limite laminaire est examiné théoriquement. L'analyse est d'abord conduite en général pour n'importe quel écoulement arbitraire d'une vapeur et d'un gaz non condensable, et certains résultats généraux sont obtenus. On trouve numériquement et par une méthode intégrale des solutions des équations différentielles de similitude. La formulation générale est appliquée au système vapeur d'eau–air et l'on compare les transports de chaleur avec et sans le gaz non condensable dans une large gamme de conditions d'essai. Les réductions de transport de chaleur dues au gaz non condensable sont accentuées lorsque la pression est faible. En général, la condensation avec convection forcée est beaucoup moins sensible que dans le cas d'un écoulement dû à la pesanteur. L'effet d'une résistance interfaciale (c'est-à-dire un saut de température à l'interface liquide–vapeur) est également examiné. Les résultats due calcul montre que l'effet sur le transport de chaleur es négligeable.

Zusammenfassung—Der Einfluss eines nichtkondensierbaren Gases auf Kondensationsvorgänge in laminarer Grenzschicht bei Zwangskonvektion wird analytisch untersucht. Die Analyse wird erst in allgemeiner Form durchgeführt für beliebige Strömung eines Dampfes und eines nichtkondensierbaren Gases; dafür wurden bestimmte universelle Ergebnisse erhalten. Lösungen der Differentialgleichungen wurden sowohl numerisch als auch nach einer Integralmethode gefunden. Die allgemeine Formulierung wird angewendet auf das Dampf–Luft-System. Der Wärmeübergang ohne und mit nichtkondensierbarem Anteil wird in einem grossen Anwendungsbereich verglichen. Die Abnahme des Wärmeübergangs infolge eines nichtkondensierbaren Anteils zeigt sich besonders bei kleinen Arbeitsdrücken. Im allgemeinen ist die Kondensation bei Zwangskonvektion weit weniger empfindlich als bei natürlicher Konvektion. Der Einfluss eines Grenzflächenwiderstandes (d.h. ein Temperatursprung an der Flüssigkeits- und Dampfgrenze) wird ebenfalls untersucht. Die errechneten Ergebnisse zeigen einen vernachlässigbaren Einfluss auf den Wärmeübergang.

Аннотация—Аналитически исследовано влияние неконденсирующегося газа на конденсацию при вынужденной конвекции в ламинарном пограничном слое. Проводился общий анализ для произвольного потока, состоящего из пара и неконденсирующегося газа, и получены некоторые общие результаты. Дифференциальные уравнения подобия решены численно, а также с помощью интегрального метода. Общая формулировка применяется для системы пар-воздух; процессы теплообмена при наличии и отсутствии неконденсирующегося вещества сравниваются между собой для широкого диапазона рабочих условий. Подчеркивается, что при низких рабочих давлениях присутствие неконденсирующегося газа снижает интенсивность теплообмена. В общем, конденсация при вынужденной конвекции гораздо менее чувствительна, чем конденсация в гравитационном потоке. Исследовано также влияние сопротивления на поверхности раздела (то есть, температурный скачок на поверхности раздела жидкость-пар). Вычисленные результаты показывают незначительное влияние сопротивления на теплообмен.